

*Research article*

## **The effect of CdO–ZnO nanoparticles addition on structural, electrical and mechanical properties of PVA films**

**Chaitra Srikanth, Gattumane Motappa Madhu\*, Hemanth Bhamidipati and Siddarth Srinivas**

Department of Chemical Engineering, M S Ramaiah Institute of Technology, MSR Nagar, Bangalore, 560054, Karnataka, India

\* **Correspondence:** Email: [gmmadhu@gmail.com](mailto:gmmadhu@gmail.com); Tel: +919845381349; Fax: +9108023603124.

**Abstract:** Cadmium oxide doped zinc oxide (CdO–ZnO) nanoparticles were synthesized by solution combustion technique. CdO–ZnO nano particles were used as fillers and their concentration ranged between 0.5% to 2.5% by weight in polyvinyl alcohol (PVA) films. The effect of nano filler concentration on structural, electrical and mechanical properties was investigated. Dielectric constant values decreased upto 1.24 GHz frequency, between 1.24 to 3 GHz frequency range a slight increase in dielectric constant was observed. At frequencies above 500 kHz increase in AC conductivity and loss tangent of the polymer nanocomposites were observed. Enhanced mechanical properties were observed with increase in dopant concentration. A significant increase of 152.65% in film toughness, 113.58% increase in elastic modulus and 83.10% increase in ultimate tensile strength was observed at 2.5 wt% concentration of CdO–ZnO in PVA film as compared to pristine PVA film, which makes CdO–ZnO a desirable reinforcing material for nanocomposites.

**Keywords:** polymer nanocomposites; SEM; XRD; dielectric constant; dielectric loss; ultimate tensile strength; elastic modulus; toughness

---

### **1. Introduction**

Polymer composite films are gaining importance in recent research especially in fabrication of nano polymer composites due to their high elasticity, high aspect ratio and specific surface area. All these properties can be achieved when a corrosion resistant, environmentally biodegradable, non-toxic, highly flexible polymer matrix is incorporated with the composite material to yield the desired polymer matrix composite. Selection of appropriate matrix and reinforcement material is an

important step, as the choice of both the materials decides the kind of polymer nanocomposite it yields. Hence, a water-soluble, biodegradable, non-toxic and easily compatible polyvinyl alcohol was chosen as the matrix material to produce polymer composite films of interest [1–7].

Researchers have found that optical band gap of CdO ranges from 2.15 to 2.7 eV.  $\text{Cd}^{2+}$  has an ionic radius of 0.095 nm. ZnO has large band gap ranging from 3.15 to 3.4 eV. Zn has an ionic radius of 0.074 nm [8,9]. Hence, doping ZnO into CdO increases the optical band width and electrical conductivity of the parent material by also retaining its crystal lattice parameters. CdO and ZnO can be used as transparent conducting oxide which can be used for preparing thin films. These polymer composite films enable us to learn the various structural, chemical and electrical properties of the composites. Therefore, mixed metal oxides have received considerable attention as nanocomposite fillers, especially cadmium oxide doped zinc oxide (CdO–ZnO) due to its use in various applications such as solar cells, photo voltaic solar cells, gas sensors, UV lasers, transparent electrodes and other optoelectronic applications [8–11].

CdO–ZnO nanopowder and polymer composite films have been synthesized and studied by different techniques earlier. Ahmad et al. [12] synthesized crystalline hexagonal CdO–ZnO nanocones by hydrothermal process and it was fabricated on a dye sensitized solar cell. The cell efficiency with the variation of other electrical parameters were calculated and reported. Rajput et al. [13] synthesized CdO–ZnO polymer composite films using zinc acetate dihydrate, cadmium acetate dihydrate along with 2-methoxy ethanol and mono ethanol amine for casting films by sol gel process and further fabricated these polymer composite films by spin coating technique and studied the oxygen gas sensing ability of these films. Sharma et al. [14] deposited CdO–ZnO composite films on a glass substrate using corresponding metal nitrates and ammonia liquor as a precursor by chemical bath deposition technique for ethanol gas sensing application. It was found that, CdO–ZnO sensor was successful in sensing ethanol gas even at very low ethanol concentration. Aruna et al. [15] found that solution combustion technique is a relatively cost effective, easier method to obtain crystalline, homogenous products. Hence, it is a preferred method for the synthesis of metal oxides and mixed metal oxides at relatively low ignition temperatures around 400 °C. CdO was incorporated in PVA films and analysed for structural, electrical and mechanical properties [16]. The results showed that with increase in doping concentration mechanical properties such as % elongation and tensile strength enhanced. Whereas, electrical properties such as AC conductivity and loss tangent increased with increase in frequency. Similar results were obtained when ZnO was incorporated into PVA films [17]. Both mechanical as well as electrical properties were enhanced. This prompted us to experiment with synthesis of mixed metal oxide, i.e, CdO–ZnO nanopowder and use it as a nano filler in PVA film and study the electrical and mechanical properties of these polymer nanocomposites.

The present work is aimed at synthesis of CdO–ZnO nanoparticles by solution combustion technique. The main objective of our work is to disperse these nanoparticles into PVA polymer matrix to obtain transparent polymer composite films by solution intercalation technique. The effect of addition of CdO–ZnO nanoparticles with varying concentrations into PVA has so far been unexplored in the field of research and remains our area of interest. For the first time, an attempt has been made to reinforce CdO–ZnO nanoparticles in PVA matrix, the electrical and mechanical properties have been estimated. Hence, we have prepared polymer composite films and characterized for various properties such as structural, electrical and mechanical properties. Structural properties were found out using Scanning Electron Microscope (SEM) and X-ray Diffractometer (XRD).

Chemical properties were analysed using Fourier Transform Infra-Red Spectroscopy (FTIR). Dielectric behaviour of the polymer composite films (PVA/CdO–ZnO) were analysed using an impedance analyser. Electrical properties such as dielectric constant ( $\epsilon'$ ), electrical conductivity ( $\sigma_{ac}$ ) and  $\tan\delta$  were calculated. Mechanical properties such as tensile strength, elastic modulus and toughness were found using Universal Testing Machine (UTM).

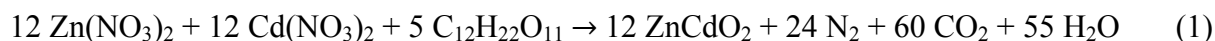
## 2. Materials and methods

### 2.1 Chemicals

Cadmium nitrate tetra hydrate was obtained from M/s S.D. Fine chemicals, molecular weight and purity for cadmium nitrate were 308.47 g/mol and 99%, respectively. Zinc nitrate hexa hydrate was procured from M/s Merck specialities. Molecular weight and purity for zinc nitrate hexa hydrate were 297.49 g/mol and 99%, respectively. PVA powder LR grade was obtained from M/s. Thomas Baker chemicals, having an approximate molecular weight of 14000. Edible sugar was used as a fuel for the solution combustion reaction. Double distilled water was used for the synthesis of CdO–ZnO nano powder and PVA synthesis.

### 2.2 Synthesis and characterization of CdO–ZnO nanoparticles

CdO–ZnO nano powder was synthesized by solution combustion method. Cadmium nitrate tetra hydrate and zinc nitrate hexa hydrate were used as metal oxidizers and domestic sugar was used as a fuel. An aqueous solution was prepared by dissolving 30 g of zinc nitrate hexa hydrate, 31.2 g of cadmium nitrate tetra hydrate and 14.3 g of domestic sugar in 90 mL of double distilled water. Cadmium to zinc ratio was maintained at 1:1 molar ratio. The fuel to metal nitrate mole ratio was 0.23. The aqueous solution was heated on a hot plate at 300 °C for 30 min. As the mixture started to boil, oxides of carbon, nitrogen and water vapour were released. This reaction resulted in the formation of a gel. As the heating continued, self-ignition of the gel occurred leading to the formation of a soft, porous, nano crystalline powder. Once the nano powder was obtained, it was calcined in a muffle furnace at 600 °C for one hour. The overall stoichiometric reaction can be represented as shown below in Eq 1.



### 2.3 Fabrication of PVA–CdO–ZnO nano-filler PVA composite films

PVA was dissolved in double distilled water by adding 37.9 g of PVA powder into 500 mL water. The mixture was heated to 65–70 °C with constant stirring for 5–6 h using a temperature controlled heater cum magnetic stirrer. The clear PVA solution was cooled to room temperature followed by ultrasonication (200 W) for 45 min, later it was poured onto a clean glass mould. The casted film was allowed to dry at room temperature for 60–72 h. PVA–CdO–ZnO nanocomposite was casted by solution intercalation technique [18]. Similar procedure was carried out for casting films of varying amounts of 0.5, 1.0, 1.5, 2.0 and 2.5% by weight of CdO–ZnO nano powder. The resultant films were found to exhibit uniform distribution of CdO–ZnO nano powder in PVA matrix

and the composite films were free from air bubbles. The film thickness was measured using LCD digital Vernier callipers and was observed to be in the range of 0.13 to 0.16 mm.

#### 2.4 Characterization techniques and measurements

Electrical properties can be better understood by initially understanding the morphological nature and other structural properties of the synthesized films. Hence, the effect of filler (CdO–ZnO) concentration on PVA matrix was analysed using SEM, XRD and FTIR. FTIR spectra for the samples was obtained using Bruker Alpha Fourier transform infrared spectrometer (FTIR) in transmittance mode in the spectral range of 4000–500  $\text{cm}^{-1}$  and a resolution of 4  $\text{cm}^{-1}$ . XRD data was obtained using PANalytical powder X-ray Diffractometer. Cu- $\alpha$  radiation (45 kV, 30 ma) was used as the X-ray source. XRD analysis was carried out for powder/polymer composite films and the results were recorded in the range of 0° to 60° at a speed of 1.8°/min at a wavelength of 1.5418 Å. Surface morphological features were analysed using Scanning Electron Microscope (SEM, TESCAN Vega 3 LMU model). Cascade Microtech PM5 Key Sight B1500A semiconductor analyser along with high frequency impedance analyser (Agilent 4294A) was used for electrical characterization of polymer composite films and the frequency ranged from 1 KHz to 1 GHz. KIPL-PC 2000 UTM (universal testing machine) was used for the mechanical properties testing of all the synthesized films. The test speed was carried out at 10 mm/min using tensile flat surface grips. ASTM D638 standard procedure was followed for performing tensile tests. Load cell was set at 0.2KN. The film thickness and width were in the range of 0.13 to 0.16mm and 15–17 mm, respectively. The error range of testing equipment was found to be  $\pm 0.2$  MPa.

### 3. Results and discussion

#### 3.1 X-ray diffraction analysis (XRD)

XRD graph of CdO–ZnO nanoparticles is as shown in Figure 1a. It consists of diffraction peaks related to CdO and ZnO indicated by circle and diamond shape respectively. The results revealed formation of CdO with cubic phase whereas ZnO was found to exist in hexagonal phase. Presence of various sharp peaks indicated that pristine CdO–ZnO exhibited crystalline nature. Zinc oxide diffraction peaks were observed at  $2\theta = 31.67^\circ, 34.33^\circ, 36.13^\circ, 47.40^\circ, 56.41^\circ$  and  $62.70^\circ$  which are associated with (100), (002), (101), (102), (110) and (103) planes. Cadmium oxide diffraction peaks were obtained at  $2\theta = 33.0^\circ, 38.30^\circ, 55.29^\circ, 65.93^\circ$  and  $69.25^\circ$  which are associated with (111), (200), (220), (200) and (222) planes, respectively. All the diffraction peaks obtained for hexagonal phase of ZnO can be assigned with lattice constants  $a = 0.325$  nm,  $c = 0.521$  nm and cubic phase of CdO can be assigned with the lattice constant  $a = 0.469$  nm. All the diffraction peaks obtained for CdO, ZnO and the (h k l) values are in good agreement with the literature values [19,20] as well as JCPDS file number 36–1451 for ZnO and JCPDS file number 05–0640 for CdO. Size of the crystallite ( $t$ ) was calculated using Debye–Scherrer formula [20] as shown below in Eq 2.

$$t = 0.9\lambda/\beta\cos\theta \quad (2)$$

where  $\lambda$  is the wavelength of the X-ray source used (0.15418 nm for Cu k-alpha),  $\beta$  is the full width at half maximum and  $\theta$  is the angle of diffraction. The smallest and largest particle size were found

to be 24.62 and 56.25 nm, respectively. The average particle size of CdO–ZnO nanopowder was found to be 36.787 nm.

XRD data of pristine PVA and PVA doped with 0.5, 1.0, 1.5, 2.0 and 2.5% by weight (wt%) CdO–ZnO nanoparticles respectively are as shown in Figure 1b. Pristine PVA and PVA doped with varying concentrations of CdO–ZnO revealed a prominent peak at  $2\theta = 19.4^\circ$  indicating a (1 0 1) crystal lattice orientation of polyvinyl alcohol [21]. XRD indicates that PVA is a semi-crystalline polymer [21]. The semi-crystalline property of the polymer was due to strong molecular interaction between the polymer networks. Similar peaks for all the doped PVA composites approximately at  $19.4^\circ$  were observed except for 2 and 2.5 wt% loading of CdO–ZnO in PVA, as the peak becomes sharp, narrow and split into two thus suggesting a better crystallinity of the PVA component probably induced by the CdO–ZnO nanoparticles. This clearly indicated the presence of CdO–ZnO nano filler in PVA matrix. As the filler concentration increases prominent peaks were observed. This could be due to increase in the crystallinity of the PVA composite material which is caused by the interaction of CdO–ZnO nano particles with the polymer chains of PVA [21].

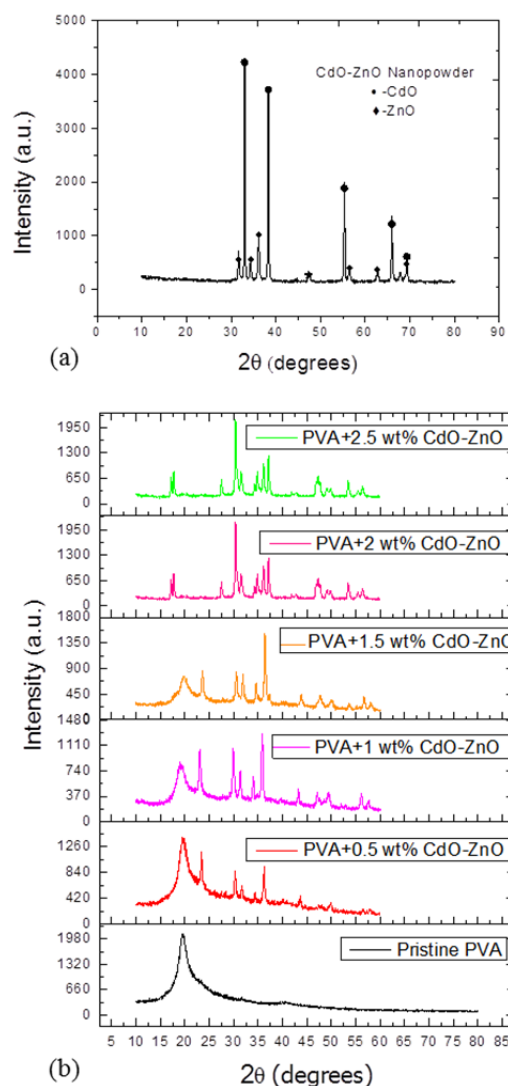


**Figure 1.** (a) XRD pattern of CdO–ZnO nano powder, (b) XRD pattern of pristine PVA film and CdO–ZnO nano powder doped PVA thin films.

### 3.2 Scanning electron microscopy (SEM)

Figure 2 reveals the surface morphological features of CdO–ZnO nano-powder. The magnified image of CdO–ZnO nano-powder (70400 $\times$ ) reveals a porous morphology, where spherical particles are agglomerated and give rise to a web-like organisation. The mean particle size of CdO–ZnO nanoparticle appears to be around 40 nm whereas, the agglomerated cluster appears to be of size 130 nm. Figure 3 shows the magnified SEM images (3000 $\times$ ) of (a) pristine PVA, (b) PVA-0.5 wt% CdO–ZnO, (c) PVA-1 wt% CdO–ZnO, (d) PVA-1.5 wt% CdO–ZnO, (e) PVA-2 wt% CdO–ZnO, (f) PVA-2.5 wt% CdO–ZnO. It can be clearly interpreted that all the polymer nano composite films are found to be agglomerated at the corners. This is due to the difference in density of PVA and CdO–ZnO nanoparticles. Since, PVA is denser than CdO–ZnO nano-particle, with increase in nano-filler concentration the level of agglomeration also keeps on increasing. Figure 3f exhibits highest level of agglomeration it is clearly visible in the form of clusters. This may be possibly due to decrease in inter-particle distance. The smallest and the largest nanoparticle in the PVA doped film were found to be 200 nm and 1  $\mu\text{m}$ , respectively.

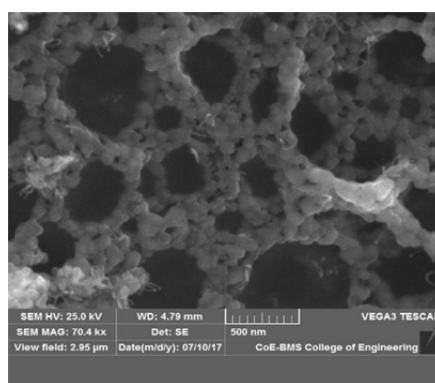


**Figure 2.** SEM image of CdO–ZnO nano-powder (70400 $\times$ ).

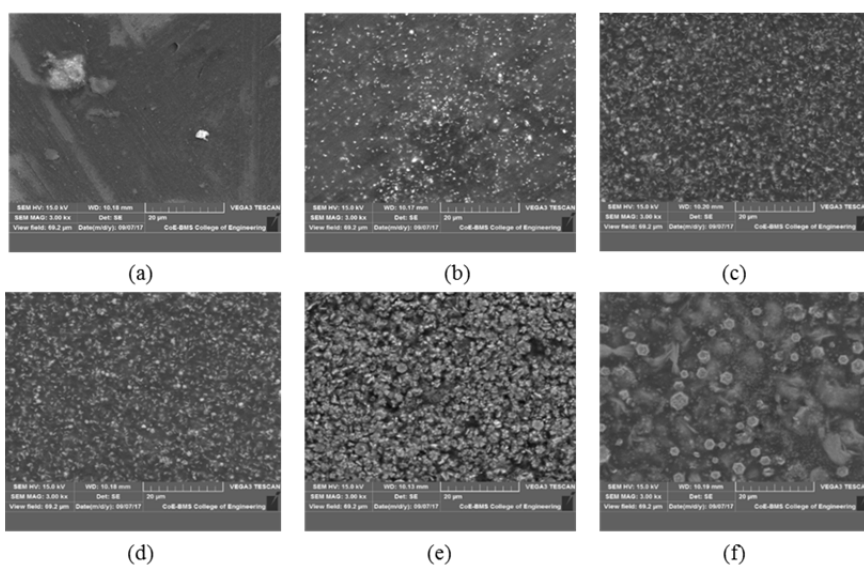


**Figure 3.** SEM images of PVA loaded with CdO–ZnO nanoparticles at (a) 0 wt%, (b) 0.5 wt% (c) 1 wt%, (d) 1.5 wt%, (e) 2 wt% and (f) 2.5 wt% (3000 $\times$ )

### 3.3 Fourier transform infrared spectroscopy (FTIR spectra)

FTIR spectra was used to analyse the interaction of CdO–ZnO nanoparticles with PVA. Three prominent peaks at 435, 466 and 502  $\text{cm}^{-1}$  were observed in CdO–ZnO nanopowder as indicated in Figure 4a. These peaks indicated the presence of CdO–ZnO and confirmed by the literature values [22–24]. Figure 4b shows the FTIR spectra of pristine PVA film and CdO–ZnO nanoparticles incorporated in PVA films respectively. Several well-defined peak bending was observed at 505, 840, 1089, 1429, 2925 and 3208  $\text{cm}^{-1}$ . The absorption band obtained in the range of 500–515  $\text{cm}^{-1}$  and 820–840  $\text{cm}^{-1}$  is mainly due to the metal oxygen vibrational stretching bond which confirms the presence of CdO–ZnO nanoparticles [22–24]. The peak obtained at 1089  $\text{cm}^{-1}$  confirms C–O–C stretching of acetyl group on PVA backbone. The absorption band at 1429 indicates C–H bending of  $-\text{CH}_2$  bond present in the PVA backbone [25]. Whereas, absorption band obtained in the range of 2919 to 2925  $\text{cm}^{-1}$  was due to C–H asymmetric stretching [25]. The strong absorption band obtained in 1300–1330 was due to vibrational stretching of O–H group [25]. No additional absorption bands were observed having a different functional group which indicates that the synthesized CdO–ZnO was in its purest form.

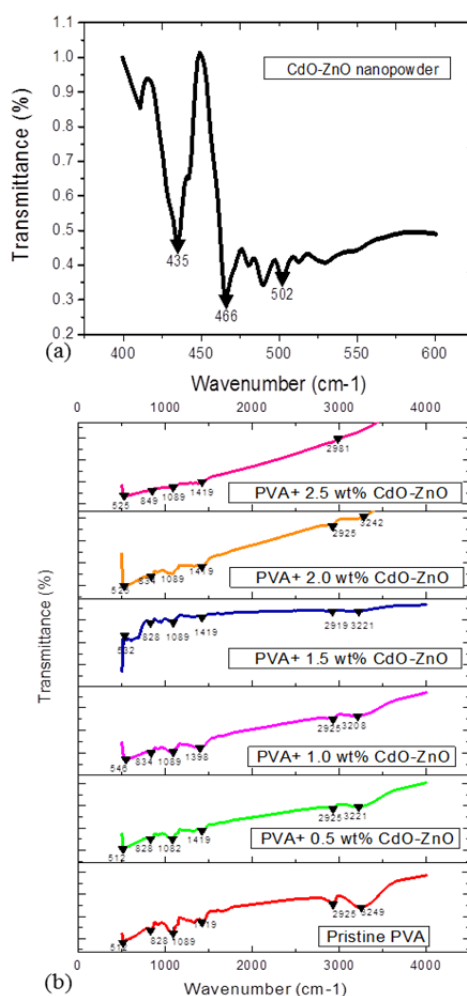


**Figure 4.** (a) FTIR spectra of CdO–ZnO nanopowder, (b) FTIR spectra of pristine PVA film and CdO–ZnO nanoparticles incorporated in PVA films.

### 3.4 Effect of CdO–ZnO nanoparticle concentration on different electrical properties of PVA matrix

#### 3.4.1 Dielectric constant

Dielectric permittivity for a composite material is determined by the combined permittivity of the matrix as well as the reinforcement. In the present work, PVA is chosen as the matrix material and reinforced with CdO–ZnO nanoparticles. Interfacial polarizations are most likely to occur, since the synthesized nanocomposites have large volume fraction of interfaces. It has been observed that, whenever insulating metal oxides are used as nanofiller the base polymer is found to exhibit a higher permittivity value compared to that of the nanocomposite [25–30].

The dielectric permittivity for a nanocomposite material can be expressed in a complex form. The real part and the imaginary part, both being a function of frequency as shown in Eq 3 [25]:

$$\varepsilon^*(\omega) = \varepsilon'(\omega) - i\varepsilon''(\omega) \quad (3)$$

where  $\varepsilon'(\omega)$  is the real part and is called as dielectric constant. It is also used to calculate capacitance of a material under an applied electric field. Whereas,  $\varepsilon''(\omega)$  is the imaginary part referred as dielectric loss. It is used to calculate the energy loss and loss tangent or  $\tan\delta$  for an applied electric field.

Dielectric constant was calculated using Eq 4:

$$\varepsilon'(\omega) = \frac{C.t}{A.\varepsilon_0} \quad (4)$$

where  $t$  is the film thickness in (m),  $C$  is equivalent parallel capacitance in [F],  $A$  is the electrode's surface area in ( $\text{m}^2$ ). The electrode's surface area and electrode diameter were found to be  $12 \times 10^{-6} \text{ m}$  and  $1.131 \times 10^{-22} \text{ m}^2$ , respectively.  $\varepsilon_0$  is the permittivity of air ( $8.85 \times 10^{-12} \text{ F/m}$ ) and  $\omega$  is the angular frequency in radians per second given by  $\omega = 2\pi f$ , and  $f$  is frequency in Hz.

The variation of dielectric constant with log frequency for PVA–CdO–ZnO nanocomposites is shown in Figure 5.

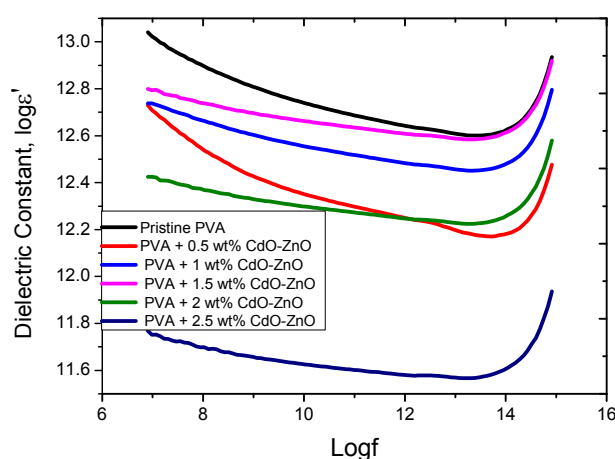


**Figure 5.** Dielectric constant of PVA–CdO–ZnO nanocomposites as a function of log frequency.



The dielectric constant ( $\epsilon'$ ) of PVA–CdO–ZnO composites decreased with increase in frequency upto 1.24 GHz. This property may be attributed due to the orientation of the dipoles in the direction of an applied field [31]. As the frequency increased beyond 1.24 GHz, it can be observed from the graph that the dielectric constant increased sharply for pristine PVA and was observed to be the least for PVA with 2.5% CdO–ZnO. This may be due to the difficulty in orientation of the larger dipolar groups at higher frequencies. Dielectric permittivity of a material depends upon various factors such as dipole number density, size of the dipolar groups and their interaction with each other. When an electric field is applied electrical charges and dipolar groups respond to electric field and reorient themselves. However, high value of dielectric constant is observed at low frequency due to the electrode effect and the interfacial phenomena occurring in the sample [32]. This verifies the fact that, for polar materials such as PVA dielectric constant shares an indirect relationship with AC frequency upto a threshold frequency of 1.24 GHz and steeply increases beyond 1.24 GHz. At low frequencies, the dielectric permittivity of CdO–ZnO nanoparticles in PVA matrix was also found to decrease with increase in frequency of the applied field [33,34]. Since, the dielectric permittivity of both PVA and CdO–ZnO nanoparticles were found to decrease with increase in frequency of the applied field hence, resulted in the decrease in dielectric constant of the PVA–CdO–ZnO polymer composite films, for increase in frequency for an applied field at low frequencies. At high frequencies, the polymer nanocomposite behaves like a semiconductor.

### 3.4.2 AC conductivity

Motion of the charge carriers in a polymer induces alternating conductivity within a sample. AC conductivity is measured using the Eq 5 [35]:

$$\sigma_{ac} = 2\pi f \epsilon_0 \epsilon \tan \delta \quad (5)$$

where  $\epsilon_0$  is the permittivity of free space (F/m),  $\epsilon$  is the real part of complex relative permittivity and  $f$  is the applied frequency (Hz).

Figure 6 illustrates the dependence of AC electrical conductivity on frequency [36]. The highest conductivity was found to be for pristine PVA with a value of  $11.27 \text{ Sm}^{-1}$ . At low frequencies the rise of conductivity was found to be negligible. In fact, up to a frequency of 500 kHz, the conductivity values remained the same for all the nanocomposite films including PVA. However, conductivity values begin to rise for frequencies higher than 500 kHz. This may be possibly due to the electronic interactions occurring within the sample leading to increase in the mobility of the charge carriers throughout the film as a result of which the samples became relatively more conductive. In PVA, as the bond rotates with increased frequency, the existing polar groups with polar bonds cause dielectric transition. This leads to a change in the chemical composition of the polymer chains due to the formation of charge transfer complexes. Hence, enhancing the flexibility of the polymer chains and a net increase in AC electrical conductivity [37].

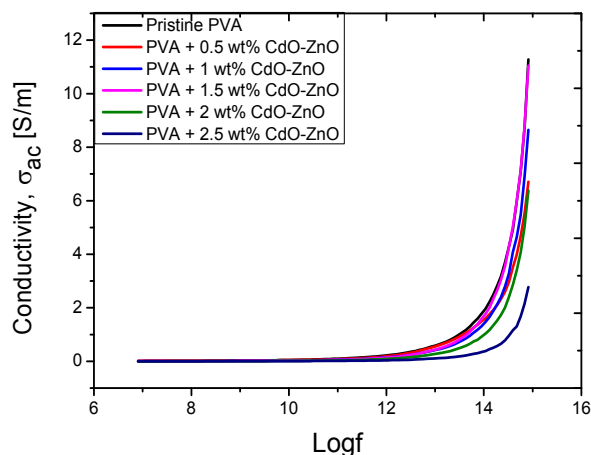


**Figure 6.** AC conductivity of PVA–CdO–ZnO nanocomposites as a function of log frequency.

### 3.4.3 Loss tangent

Loss tangent of a medium is the ratio of magnitude of imaginary part and magnitude of real part of the dielectric permittivity expressed in complex form. The loss tangent  $\tan\delta$  was determined using dielectric constant  $\epsilon'$  and dielectric loss  $\epsilon''$  from the equation  $\epsilon'' = \epsilon' \tan\delta$ , where  $\delta$  is the phase angle between the electric field and the polarization of the dielectric. Figure 7 illustrates the dependence of loss tangent of PVA–CdO–ZnO nanocomposites on frequency. It can be observed from the figure that  $\tan\delta$  decreased with increase in frequency for an applied field until a minimum at 168 kHz. As frequency increased from 500 kHz to 3 GHz,  $\tan\delta$  values were found to increase. Increase in  $\tan\delta$  values with increase in frequency indicates presence of high resistive electric current component, due to increase in loss storage ratio and hence the composite behaves as a semiconductor. The experimental results obtained indicate that  $\epsilon'$ ,  $\epsilon''$  and  $\tan\delta$  strongly depend upon frequency [38].

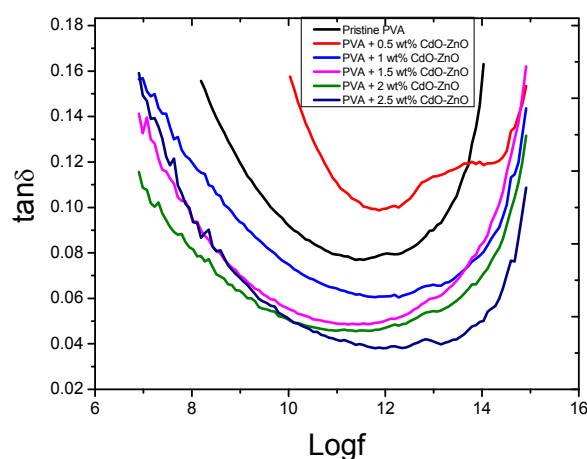


**Figure 7.** Loss tangent of PVA–CdO–ZnO nanocomposites as a function of log frequency .

### 3.4.4 Effect of nano CdO–ZnO filler concentration on electrical properties

Figure 8 shows the effect of CdO–ZnO loading on of electrical properties. Variation of all the electrical properties were recorded at room temperature. At low frequencies, the dielectric constant, dielectric loss and loss tangent were observed to be low. Whereas, at very high frequencies, especially at 3 MHz all the dielectric properties showed significant increase. This indicated that the material exhibited a typical semiconducting behaviour [16–18]. When the CdO–ZnO content is below 1 wt%, there is a slight increase in the electrical conductivity of the composite with increase in frequency. At 1.5 wt% of CdO–ZnO in PVA, all the electrical properties reached a maximum. The peak increase in electrical properties at 1.5 wt% of CdO–ZnO in PVA was due to strong bonding of the filler with the polymer molecules present in PVA. As the concentration kept on increasing beyond 1.5 wt% CdO–ZnO all the electrical properties began to decline due to the saturation level reached by CdO–ZnO content in PVA matrix. When CdO–ZnO content increased from 1.5 to 2.5 wt%, there is a transition from semi-conductor to a good dielectric [18,25]. This transition is also confirmed by low  $\tan\delta$  and the ratio of  $\epsilon''/\epsilon'$  is much less than 1. Below 1 wt% of CdO–ZnO, the material can be used in electronic devices. If the filler content is ranging from 1.5 to 2.5 wt% of CdO–ZnO, the material is well suited for simple capacitors [16–18,25].

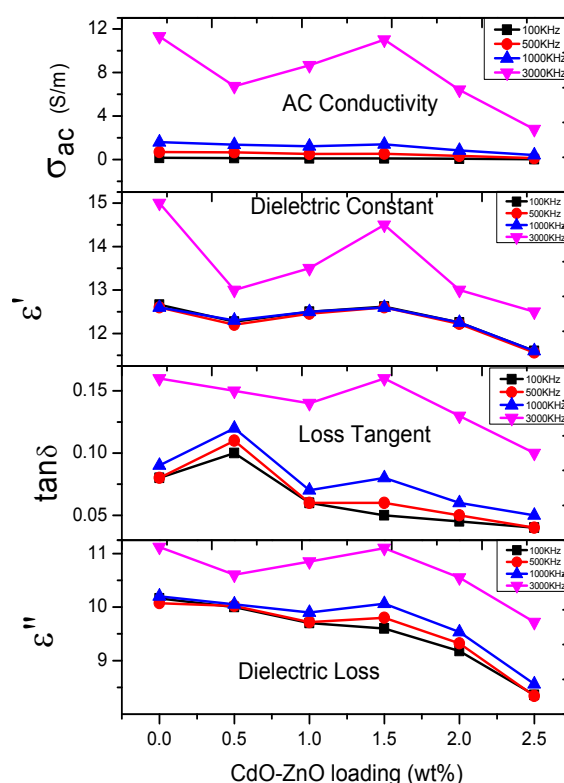


**Figure 8.** Influence of electrical properties with nano CdO–ZnO loading in PVA matrix at different frequency (100, 500, 1000, 3000 kHz).

### 3.5 Effect of CdO–ZnO nanoparticle concentration on different mechanical properties of PVA matrix

#### 3.5.1. Effect of filler loading on stress-strain relationship

The polymer composite films were initially tested to find out the stress-strain relationship as indicated in Figure 9. It can be observed from the graph that, pristine PVA has the least elongation and break even points compared to the doped samples. Increase in CdO–ZnO content in the PVA film gradually increased the tensile strength of the films, highest for PVA with 2.5 wt% CdO–ZnO. This is due to the increased molecular interaction between the CdO–ZnO nanoparticles and PVA matrix. Enhanced bonding of CdO–ZnO particles by chelation with hydroxyl groups of PVA matrix has hence resulted an increase in elongation of the break-even points.

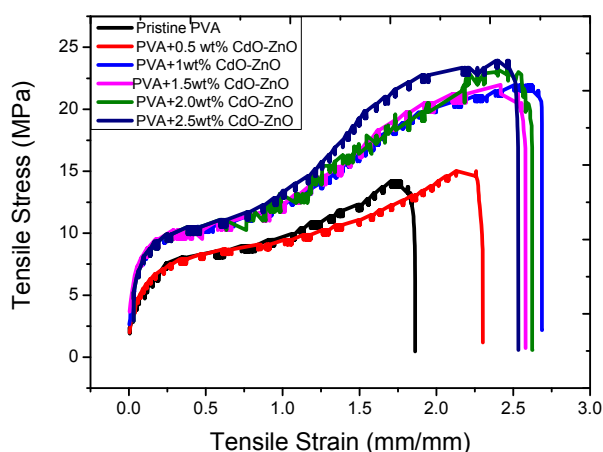


**Figure 9.** Stress-strain relationship of pristine PVA film and for varying concentrations of CdO–ZnO with PVA.

#### 3.5.2 Effect of filler loading on film toughness

Film toughness was calculated based on the area under the stress-strain curve. From Figure 10 and Table 1, it can be inferred that 2.5 wt% concentration of CdO–ZnO in PVA film exhibited the highest toughness value of 42 MPa. An exponential rise was observed for increase in filler concentration at 1 wt% this indicated a drastic increase of 152.65% in film toughness as compared to pristine PVA film. However, significant increase in toughness was not observed with further addition of nano filler in PVA matrix. Highest value of toughness was observed at 2.5 wt% concentration of CdO–ZnO in PVA film. The percentage error as shown in Figure 10 varied from 1% to 3%.

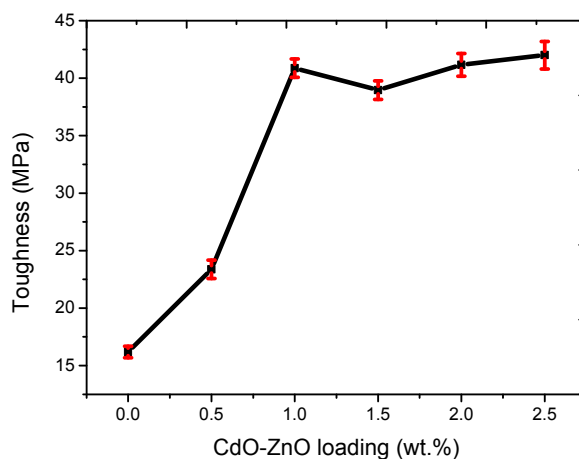


**Figure 10.** Effect of CdO–ZnO content on film toughness.

**Table 1.** Effect of CdO–ZnO content on various mechanical properties of films.

CdO–ZnO content (wt%)	Elastic Modulus (MPa)	Increase in Elastic Modulus (%)	Increase in Toughness (MPa)	Increase in toughness (%)	Peak load at break point (N)	Ultimate Tensile Strength (MPa)	Increase in ultimate tensile strength (%)
0.0 <sup>a</sup>	16.2	-	16.18	-	29.4	14.2	-
0.5	19.4	19.75	23.37	44.44	37.3	15.0	5.63
1.0	22.1	36.42	40.88	152.65	49.0	21.9	54.22
1.5	22.6	39.50	38.96	140.80	29.4	22.0	54.92
2.0	24.5	51.23	41.16	154.39	40.2	23.9	68.31
2.5	34.6	113.58	42	159.57	40.2	26	83.10

\*<sup>a</sup> Refers to Pristine PVA film.

### 3.5.3 Effect of filler loading on ultimate tensile strength

Ultimate tensile strength of all the polymer composite films with varying nano filler concentrations are as shown in Figure 11. It can be observed from the graph that doping concentration showed a linear increase of ultimate tensile strength. The highest ultimate tensile strength was found to be for PVA with 2.5 wt% CdO–ZnO. As sharp increase of 83.1% in ultimate tensile strength for 2.5 wt%. Loading of CdO–ZnO into PVA matrix indicated an effective cross-linking between the nano fillers and the PVA matrix, which contributed to excellent enhancement in the ultimate tensile strength of the films. The percentage error as shown in Figure 11 varied from 0.75% to 3%.

The increase in toughness and ultimate tensile strength could possibly be attributed due to enhanced surface morphological features and enhanced interfacial interaction between the nano particles and PVA matrix.

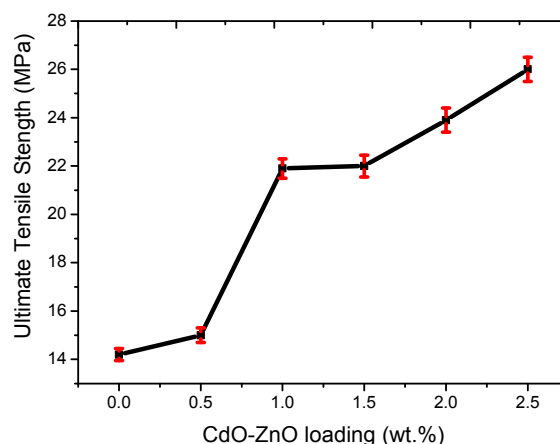


**Figure 11.** Effect of CdO–ZnO content on the ultimate tensile strength of the film.

#### 3.5.4 Effect of filler loading on Elastic Modulus

Figure 12 shows the effect of CdO–ZnO content on the elastic modulus of the film. Increase in filler loading into PVA matrix showed a gradual increase in the elastic modulus up to 2 wt%. The film elasticity increased to 51.23% at 2 wt% of CdO–ZnO in PVA as compared to pristine PVA film. With further addition at 2.5 wt% of CdO–ZnO in PVA a drastic increase in elastic modulus of 113.58% was observed in comparison with pristine PVA film, which indicated that percentage increase in the elastic modulus doubled when the concentration increased from 2 to 2.5 wt% of CdO–ZnO in PVA matrix. This is mainly due to the reduction in the strain component which has led to a drastic increase in the film elasticity. This clearly shows the role of CdO–ZnO nanoparticles in improving the film stiffness and good load bearing capacity due to strong inter-particle adherence between the PVA matrix and the nano filler. The percentage error as shown in Figure 12 varied from 1.5% to 3%.

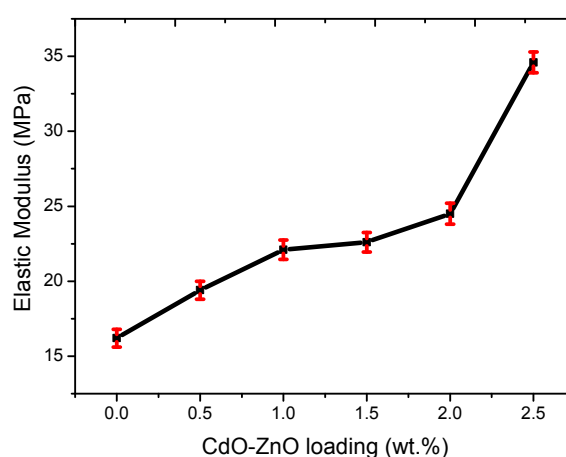


**Figure 12.** Effect of CdO–ZnO content on the elastic modulus of the film.

#### 4. Conclusion

CdO–ZnO nano material was synthesized by solution combustion method and reinforced into PVA matrix by solution intercalation technique. Effect of variation of filler content on polymer composite films were studied. Structural characterization of the nanopowder and the films showed the detailed morphology, crystallinity and the metal oxide interactions in the compound. Electrical results revealed that, dielectric constant,  $\tan\delta$  and AC conductivity increased with increase in frequency and reached a maximum at 1.5 wt% CdO–ZnO in PVA, later decreased with increase in nano filler content. Electrical results indicated that PVA–CdO–ZnO nanocomposite films can be used for insulation applications at low frequencies ranging from 1 kHz to 1.25 MHz and at high frequencies around 1.25 to 3 MHz it is best suited for semiconductor applications. Mechanical results revealed that the ultimate tensile strength almost doubled at 2.5 wt% CdO–ZnO in PVA as compared to pristine PVA. Highest toughness was observed for 2.5 wt% CdO–ZnO in PVA with a remarkable increase of 159.57% in its toughness value. Steep increase in elastic modulus for 2.5 wt% CdO–ZnO in PVA was observed. These results indicate that at 2.5 wt% CdO–ZnO in PVA, superior films with enhanced mechanical properties can be obtained and are promising materials for nano-technological applications in future.

#### Acknowledgements

The authors are very grateful to Department of Science and Technology, New Delhi, India, for providing financial assistance under Women Scientist A-Scheme to carry out the entire project work. Project Sanction No. SR/WOS-A/ET-16/2017. They are also thankful to Department of Chemical Engineering, MSRIT, Bangalore, for the technical support to carry out the research work. Electrical testing was performed at CeNSE lab, IISC, Bangalore.

#### Conflict of interests

All authors declare no conflicts of interest in this paper.

#### References

1. Ching YC, Iskandar I (2011) Effect of polyurethane/nano-SiO<sub>2</sub> composites coating on thermo-mechanical properties of polyethylene film. *Adv Mater Proc* 2010 161–164.
2. Ching YC, Yun CC, Iskandar Y (2012) Weathering resistance of solvent borne polyurethane/nanosilica composite. *Adv Sci Lett* 12: 165–169.
3. Arunkumar L, Venkataraman A (2005) Polymer nanocomposites. *Resonance* 10: 49–57.
4. Ching YC, Iskandar IY (2010) Influence of nanosilica/polyurethane composite coating on IR effectiveness and visible light transmission properties of polyethylene. *Adv Mater Res* 97–101: 1669–1672.
5. Li S, Shiling Z, Shuxue Z, et al. (2011) Physical and optical properties of silica/polymer nanocomposite inverse opal. *Adv Sci Lett* 11–12: 3445–3450.
6. Ching YC, Iskandar IY (2009) Influence of nano-SiO<sub>2</sub>/polyamide composites coating on thermic effect and optical properties of polyethylene film. *Int J Mod Phys B* 23: 06n07.

7. Ranjith J, Harding I, Bowater I, et al. (2004) Preparation, surface modification and characterisation of solution cast starch PVA blended films. *Polym test* 23: 17–27.
8. Usharani K, Balu AR (2015) Structural, optical, and electrical properties of Zn-doped CdO polymer composite films fabricated by a simplified spray pyrolysis technique. *Acta Metall Sin-Eng* 28: 64–71.
9. Pathak TK, Rajput JK, Kumar V, et al. (2017) Transparent conducting ZnO–CdO mixed oxide thin films grown by the sol-gel method. *J colloid Interf Sci* 487: 378–387.
10. Trilok S, Pandya DK, Singh R, et al. (2011) Synthesis of cadmium oxide doped ZnO nanostructures using electrochemical deposition. *J Alloy Comp* 509: 5095–5098.
11. Fazhan W, Liu B, Zhijun Z, et al. (2009) Synthesis and properties of Cd-doped ZnO nanotubes. *Physica E* 41: 879–882.
12. Umar A, Akhtar MS, Al-Assiri MS, et al. (2018) Composite CdO–ZnO hexagonal nanocones: efficient materials for photovoltaic and sensing applications. *Ceram Int* 44: 5017–5024.
13. Jeevitesh KR, Trilok KP, Vinod K (2018) CdO:ZnO nanocomposite thin films for oxygen gas sensing at low temperature. *Mater Sci Eng B-Adv* 228: 241–248.
14. Sharma AK, Potdar SS, Pakhare KS, et al. (2017) The selective ethanol gas sensing performance of CdO<sub>1-x</sub>ZnO<sub>x</sub> nanocomposite. *J Mater Sci-Mater E* 28: 3752–3761.
15. Aruna ST, Alexander SM (2008) Combustion synthesis and nanomaterials. *Curr Opin Solid St M* 12: 44–50.
16. Rashmi SH, Soumyashree S, Shrusti S, et al. (2018) Structural mechanical and electrical property evaluation of nano cadmium oxide polyvinyl alcohol composites. *Int J Plast Technol* 22: 41–55.
17. Rashmi SH, Raizada A, Madhu GM, et al. (2015) Influence of zinc oxide nanoparticles on structural and electrical properties of polyvinyl alcohol films. *Plast Rubber Compos* 44: 33–39.
18. Rao JK, Abhishek R, Debargha G, et al. (2015) Investigation of structural and electrical properties of novel CuO–PVA nanocomposite films. *J Mater Sci* 50: 7064–7074.
19. Cai X, Dan H, Shaojuan D, et al. (2014) Isopropanol sensing properties of coral-like ZnO–CdO composites by flash preparation via self-sustained decomposition of metal–organic complexes. *Sensor Actuat B-Chem* 198: 402–410.
20. Sathish DV, Ch RK, Ch VR, et al. (2012) Structural and optical investigations on ZnCdO nanopowder. *Phys Scripta* 86: 035708.
21. Bhadra J, Sarkar D (2010) Electrical and optical properties of polyaniline polyvinyl alcohol composite films. *Indian J Pure Ap Phys* 48: 425–428.
22. Suzan AK, Abaker M, Ahmad U, et al. (2012) Synthesis and characterizations of Cd-doped ZnO multipods for environmental remediation application. *J Nanosci Nanotechno* 12: 8453–8458.
23. Karthik K, Dhanuskodi S, Gobinath C, et al. (2015) Microwave-assisted synthesis of CdO–ZnO nanocomposite and its antibacterial activity against human pathogens. *Spectrochim Acta A* 139: 7–12.
24. Rahman MM, Sher BK, Hadi MM, et al. (2014) Facile synthesis of doped ZnO–CdO nanoblocks as solid-phase adsorbent and efficient solar photo-catalyst applications. *J Ind Eng Chem* 20: 2278–2286.



25. Rao JK, Abhishek R, Satyanarayana SV (2016) Influence of cadmium sulfide nanoparticles on structural and electrical properties of polyvinyl alcohol films. *Express Polym Lett* 10: 883–894
26. Tanaka T (2005) Dielectric nanocomposites with insulating properties. *IEEE T Dielect El In* 12: 914–928.
27. Zhang L, Wu P, Li Y, et al. (2014) Preparation process and dielectric properties of Ba<sub>0.5</sub>Sr<sub>0.5</sub>TiO<sub>3</sub>-P(VDF-CTFE) nanocomposites. *Compos Part B-Eng* 56: 284–289.
28. Dang ZM, Yuan JK, Zha JW, et al. (2012) Fundamentals, processes and applications of high-permittivity polymer-matrix composites. *Prog Mater Sci* 57: 660–723.
29. Panda M, Srinivas V, Thakur AK (2008) On the question of percolation threshold in polyvinylidene fluoride/nanocrystalline nickel composites. *Appl Phys Lett* 92: 132905.
30. Yang C, Patricia CI, Karim Y (2004) The future of nanodielectrics in the electrical power industry. *IEEE T Dielect El In* 11: 797–807.
31. Dutta P, Biswas S, Subodh KD (2002) Dielectric relaxation in polyaniline-polyvinyl alcohol composites. *Mater Res Bull* 37: 193–200.
32. Ramadhar S, Tandon RP, Panwar VS, et al. (1991) Low-frequency ac conduction in lightly doped polypyrrole films. *J Appl Phys* 69: 2504–2511.
33. Livi A, Levita G, Rolla PA (1993) Dielectric behavior at microwave frequencies of an epoxy resin during crosslinking. *J Appl Polym Sci* 50: 1583–1590.
34. Eloundou JP (2002) Dipolar relaxations in an epoxy-amine system. *Eur Polym J* 38: 431–438.
35. Vijaya BM, Padmasuvarna R (2016) Dielectric properties of the conducting polymers based on nr, nbr using two-point method at microwave frequencies. *IJASTEMS* 2: 106–112.
36. Tripathi R, Kumar A, Sinha TP (2009) Dielectric properties of CdS nanoparticles synthesized by soft chemical route. *Pramana* 72: 969–978.
37. Bhajantri RF, Ravindrachary V, Harisha A, et al. (2007) Effect of barium chloride doping on PVA microstructure: positron annihilation study. *Appl Phys A-Mater* 87: 797–805.
38. Ho CH, Liu CD, Hsieh CH, et al. (2008) High dielectric constant polyaniline/poly (acrylic acid) composites prepared by in situ polymerization. *Synthetic Met* 158: 630–637.



AIMS Press

© 2019 the Author(s), licensee AIMS Press. This is an open access article distributed under the terms of the Creative Commons Attribution License (<http://creativecommons.org/licenses/by/4.0>)